# Supporting information to

# Mode switching and filtering in nanowire lasers

Robert Röder,[1]* Themistoklis P.H. Sidiropoulos,[2]* Robert Buschlinger,[3]* Max Riediger,[1] Ulf Peschel,[3] Rupert F. Oulton,[2] Carsten Ronning,[1]

[1] Friedrich-Schiller-University Jena, Institute of Solid State Physics, Max-Wien-Platz 1, 07743 Jena, Germany

[2] Blackett Loboratory, Imperial College London, Prince Consort Road, SW7 2BZ London, United Kingdom

[3] Friedrich Schiller University Jena, Institute of Condensed Matter Theory and Solid State Optics, Max-Wien-Platz 1, 07743 Jena, Germany

* These authors contributed equally to this work

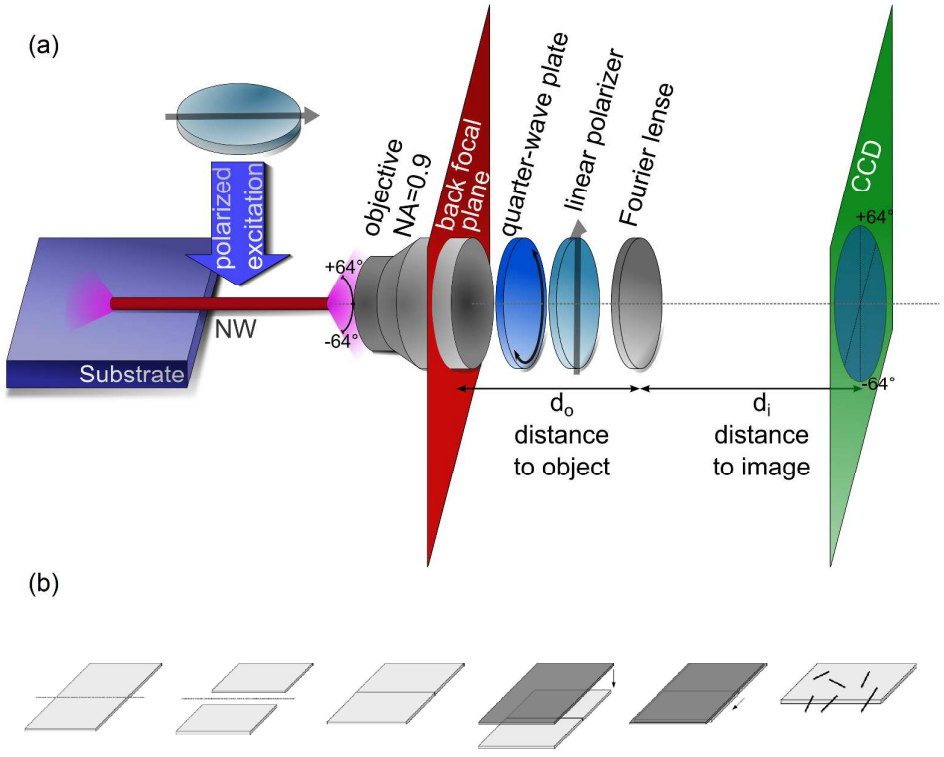


**Figure S1** (a) Schematic drawing of the 'head-on' setup for Fourier image acquisition. Excitation and detection beam paths are mutually decoupled. A quarter-wave plate and linear polarizer are used to determine the Stokes parameter S0 – S3. (b) Schematics of the modified dry imprint technique; splitting the dielectric "target" substrate and putting it together (step 1-

3), putting nanowire growth batch on top and sliding perpendicular to the edge (step 4-5), resulting sample for head-on investigations (6).

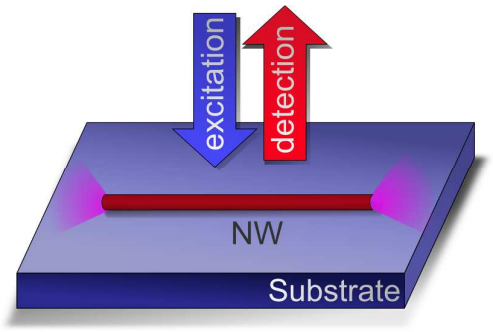


**Figure S2** Schematic drawing of a conventional micro-photoluminescence (µPL) measurement geometry in reflection.

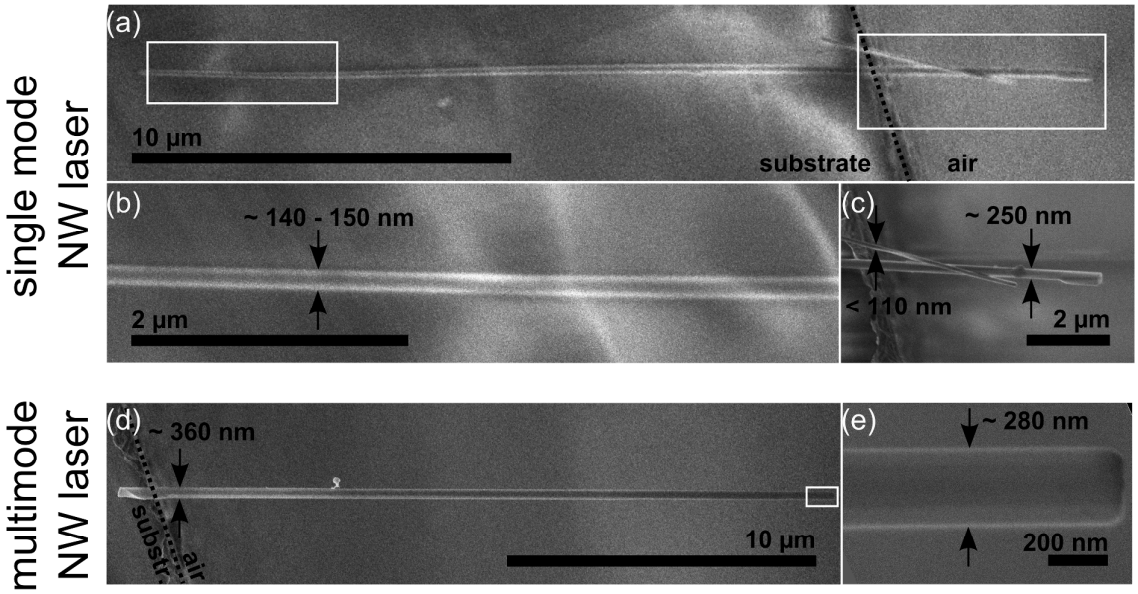


**Figure S3:** (a,b,c) Scanning electron microscopy (SEM) image of the thin single mode ZnO NW deposited at the edge of the substrate (dashed line). The relevant NW exhibits a thinnest diameter of ~140-150 nm. Additionally, a second ZnO NW lies on top of the NW, this particular NW is too thin to reveal lasing and contributes only with unpolarized spontaneous emission. (d,e) SEM image of the multimode ZnO NW with a diameter ranging from 280 – 360 nm.

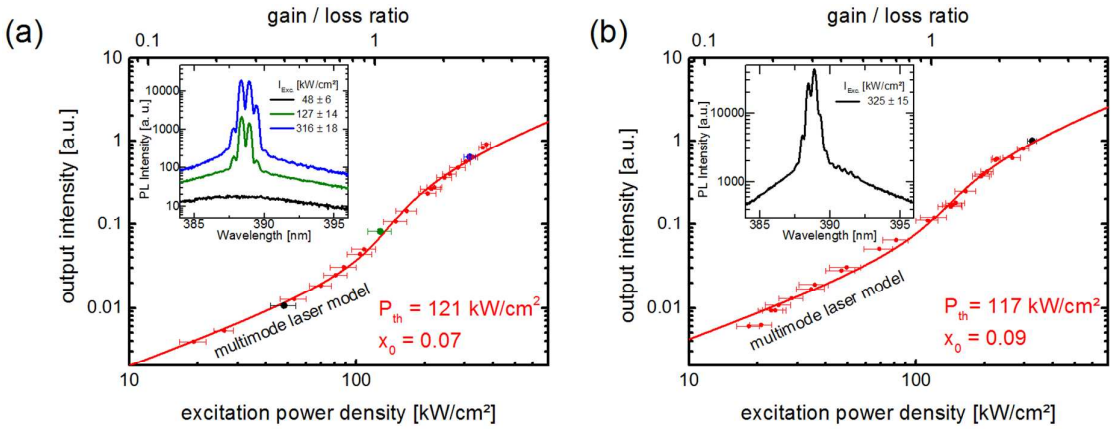


**Figure S4:** The S-shaped power dependence in the log−log plot of the output intensity data versus excitation power clearly proves lasing for the thin (a; article figure 2a-c) and the thick (b, article figure 2d-e) ZnO NW by fitting the data with a model developed for multimode laser oscillators [1] (solid lines). The insets show the respective emission spectra obtained at the given pump power. The data were acquired 'head-on' using the setup shown in Figure S1.

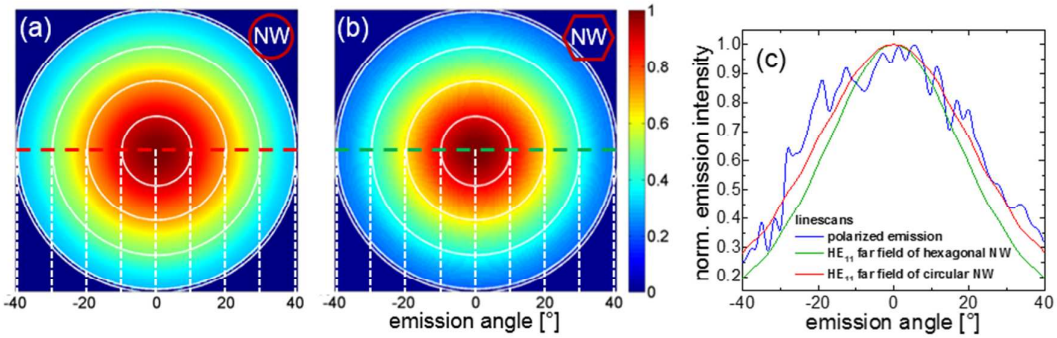


**Figure S5:** Comparison of the far field patterns simulated for a thin ~ 140 nm diameter ZnO NW with circular (a) and hexagonal (b) cross section. (c) Linescans taken from the simulated far field patterns in (a,b) coincide with the measured far field pattern (blue).

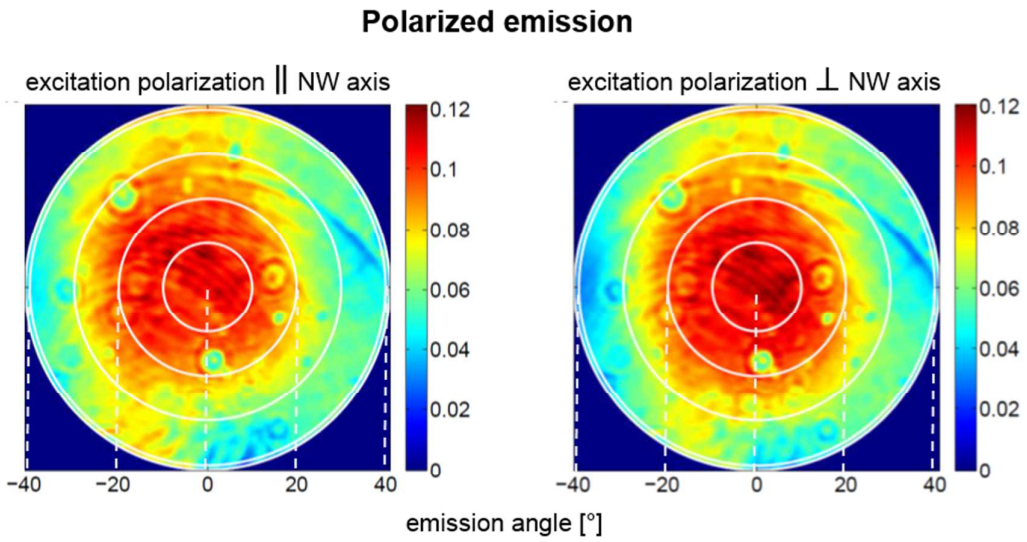


**Figure S6:** Angular resolved far field pattern of the fully polarized laser emission out of the end facet of the thin ZnO NW below the single mode cut-off , when the pump beam was applied with the polarization parallel (left) or perpendicular (right) to the NW axis. Note, although the objective enables imaging between -64° to 64°, a relative tilt of the NW to the sample edge by ~ 20° only allowed an accurate imaging from -40° to 40°.

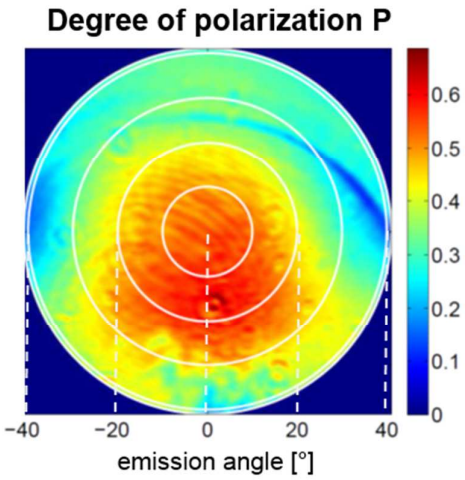


**Figure S7:** The angular resolved degree of polarization P, which was obtained by $P = \sqrt{S_1^2 + S_2^2 + S_3^2}/S_0$, reveals values around 60 – 70% at the center.

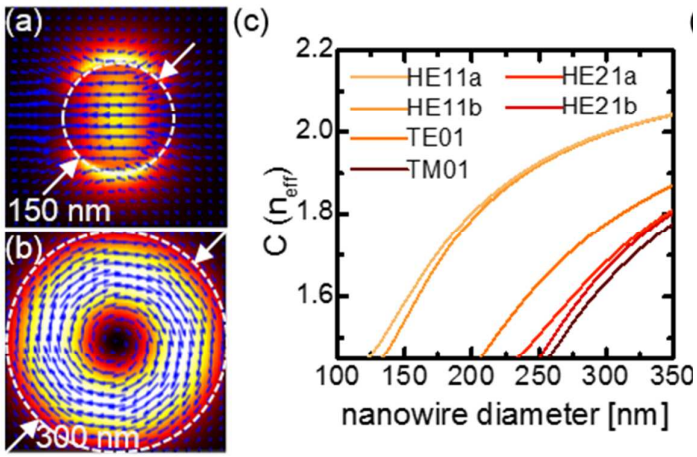


**Figure S8:** (a,b) Calculated electric field distribution of the $HE_{11b}$ mode for a 150 nm diameter ZnO nanowire and the $TE_{01}$ mode for a 300 nm diameter ZnO nanowire, respectively. (c) Effective index $n_{eff}$ as function of nanowire diameter for the lowest-order modes propagating in a ZnO nanowire with circular cross section surrounded by air and lying on a dielectric $SiO_2$ substrate. The refractive index n of ZnO was set to ~ 2.1 like in a highly excited ZnO according to [2].

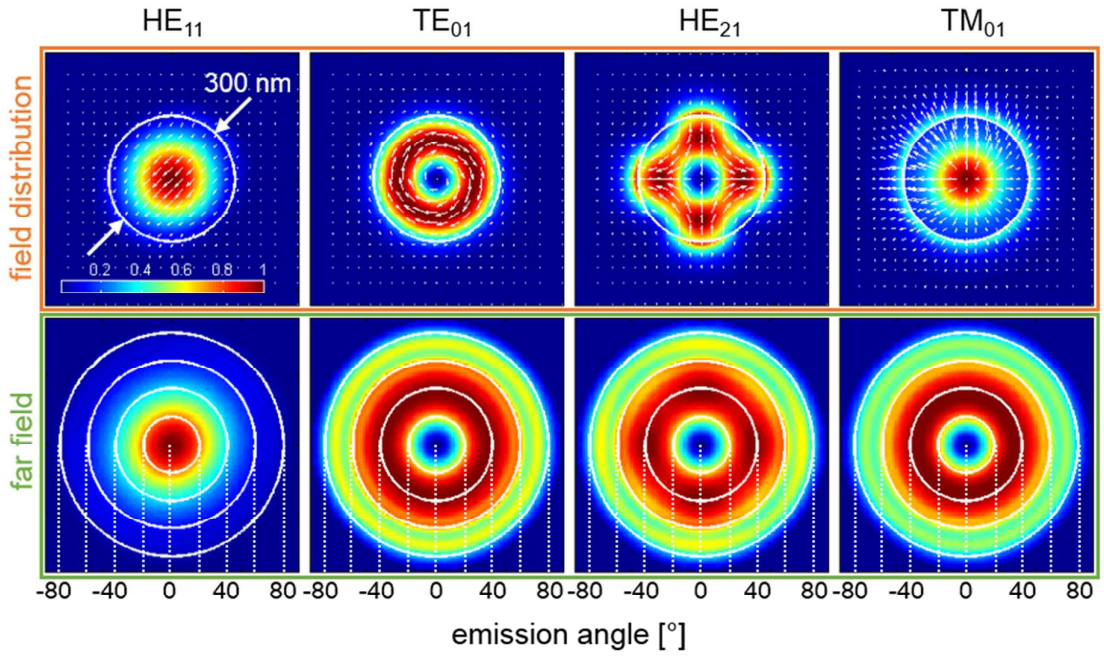


**Figure S9:** Simulated field distributions (orange, top row) and far field patterns (green, bottom row) of the first transverse modes propagating within a 300 nm diameter ZnO NW with circular cross section.

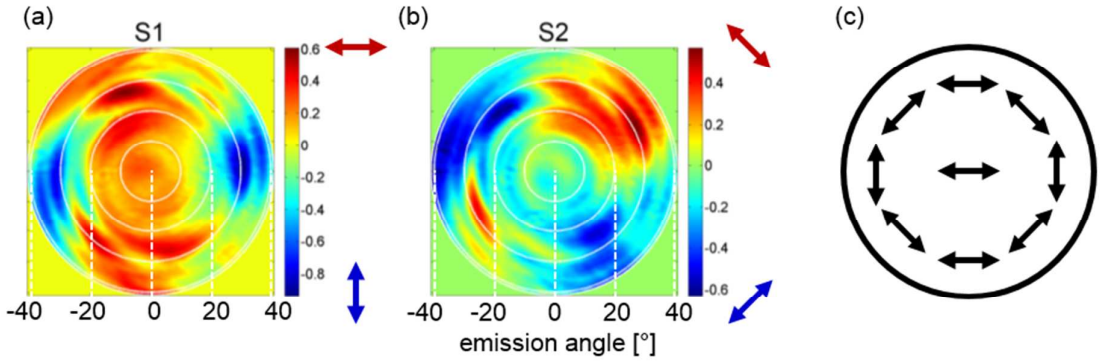


**Figure S10:** The angular resolved Stokes parameter S1 (a) and S2 (b) indicating the respective orientation of the linear polarized part of the laser emission from the thick ZnO NW. (c) The azimuthally polarized emission annulus coincides with the expectations for the $TE_{01}$ mode, while the linear polarized emission in the center indicates the admixture of the $HE_{11}$ ground mode.

**Double pump setup**

In this technique two energetically identical (355 nm, 150 fs pulse width, 800 kHz repetition rate) pump pulses separated by a time delay $\tau$ individually excite a single nanowire. The power of both pump pulses differ considerably. A strong pulse excites the nanowire at about twice its laser threshold and a weak delayed pulse is set to a fifth of the other pump pulse's power well below the lasing threshold. The measurements were performed in the reflection geometry (see figure S2) with the NWs lying completely on the dielectric substrate and for each time delay the time-integrated laser emission was recorded with a photo diode (see figure S11).

In order to excite the nanowires with two temporally separated pump pulse we use a beamsplitter to send about 45% of the incoming pump through a delay line (25 mm travel ≈160 ps long time scans) and combine both beams again using a half-mirror, **Error! Reference source not found.**11. The intensity in both beam paths can be adjusted separately by continuous OD filters. After passing through a cylindrical lens both pulses are focused onto the sample via a 20x, 0.4 NA UV microscope objective where the strong beam is at normal incident while the weak pulse excite the sample under a small angle. Here, the cylindrical lens creates an elliptical spot allowing a more efficient excitation of the nanowires

compared to a circular spot. To measure the full temporal response of our devices we modulate the weak pump and detect the time integrated signal of a photo diode with a Lock-In amplifier (Stanford Research Systems SR830).

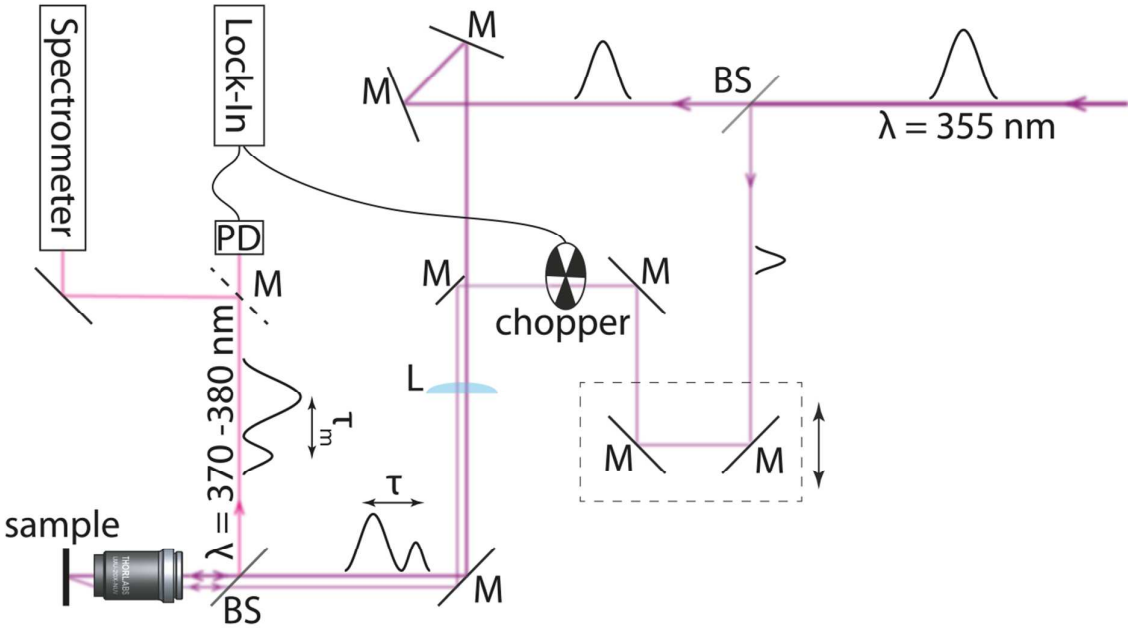


**Figure S11: Experimental double-pump setup.** The figure shows the basic setup used to measure the lasing as well as the temporal characteristics. Here, we can switch between a spectrometer to measure the lasing behavior as well as the interference between the two output pulses and a photo diode to measure the full temporal response of our devices

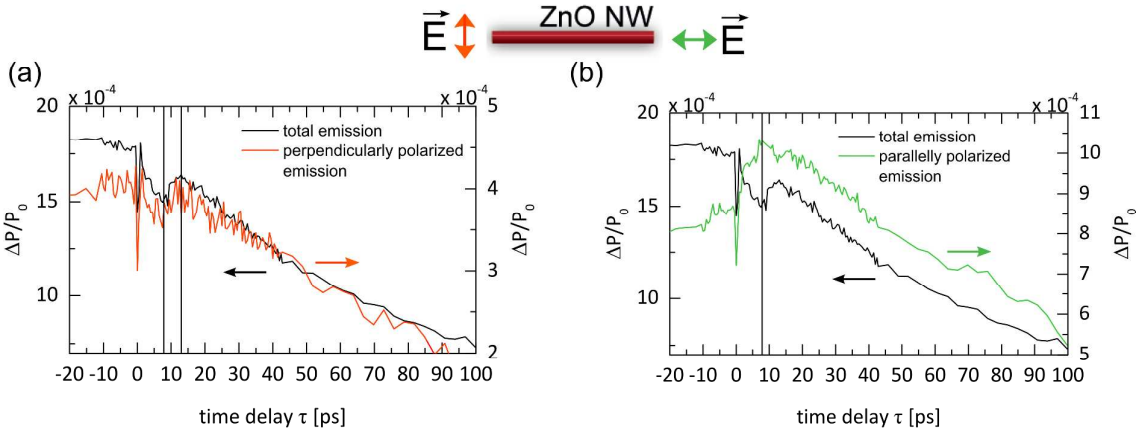


**Figure S12:** Normalized change in the laser emission $\Delta P/P_0$ when excited with two pulses separated by a time delay $\tau$ for perpendicular (a) and parallel (b) polarization. The data indicate that a thick NW was investigated here, revealing a time-integrated response with two

maxima. The maximum at larger time delays (a) is clearly polarized perpendicular to the NW axis. Thus, the slower response originates very likely from the $TE_{01}$ mode, while the faster response, which is obvious as a dip in the total output, is caused by the fundamental mode with a polarization parallel to the NW axis. The polarization resolved data strongly suggests the competition of the transversal lasing modes.

**Simulation of double-pump response**

The measured double-pump response of Fig. 4a can be simulated using a laser rate equation model as described in Ref. [3]. To account for the two lasing modes we calculate the cavity photons number for each mode separately.

$$\dot{N}_3 = RN_1 - N_3/\tau_{therm}$$

$$\dot{N}_2 = -(\Gamma_{HE_{11}}\beta_{HE_{11}}s_{HE_{11}} + \Gamma_{TE_{01}}\beta_{TE_{01}}s_{TE_{01}})s(N_2 - N_1)/\tau_m - A_0N_2 + N_3/\tau_{therm}$$

$$\dot{s}_{HE_{11}} = \Gamma_{\mathrm{HE}_{11}}\beta_{HE_{11}}s_{HE_{11}}(N_2 - N_1)/\tau_m + \beta_{HE_{11}}A_0N_2 - \gamma_{HE_{11}}s_{HE_{11}}$$

$$\dot{s}_{TE_{01}} = \Gamma_{\mathrm{TE}_{01}}\beta_{TE_{01}}s_{TE_{01}}(N_2 - N_1)/\tau_m + \beta_{TE_{01}}A_0N_2 - \gamma_{TE_{01}}s_{TE_{01}}$$

where, $N_i$ is the population of the $i$th state with a maximum of $N_T = 10^6$, $\beta_{TE_{01}} = 0.003, \beta_{HE_{11}} = 0.008$ is the spontaneous emission factor, $\tau_m = 350$ ps is the ZnO exciton lifetime, $R$ is the input pump rate, $s$ is the photon cavity number, $\gamma_{TE_{01}}^{-1} = \tau_{TE_{01}}, \gamma_{HE_{11}}^{-1} = \tau_{HE_{11}}$ is the cavity photon lifetime, $\Gamma_{TE_{01}} = 1.6, \Gamma_{HE_{11}} = 1$ is the confinment factor, and $\tau_{therm} = 1$ ps is the thermalization time.

To simulate the double-pump response for nanowires of different thickness we vary Γ and $\tau_{TE_{01}}/\tau_{HE_{11}}$ which reflects the dependency of the confinement factor and end-facet reflectivity on the nanowire diameter [4]. For thin (<150 nm) nanowires we only simulate the $HE_{11}$ mode with $\Gamma_{\mathrm{HE}_{11}} = 1, \tau_{HE_{11}} = 1.7\ ps$, for medium (~200 nm) nanowires we use $\Gamma_{\mathrm{HE}_{11}} = 1, \Gamma_{TE_{01}} = 1.4, \tau_{HE_{11}} = 2\ ps, \tau_{TE_{01}} = 7\ ps$ and for thick (>200 nm) nanowires $\Gamma_{\mathrm{HE}_{11}} = 1, \Gamma_{TE_{01}} = 1.6, \tau_{HE_{11}} = 2.5\ ps, \tau_{TE_{01}} = 10\ ps$.

By integrating the photon cavity number for all modes over the whole simulated time scale we obtain the total output, see Fig. S13a. We also assumed that in the experiment the $HE_{11}$ mode has a two times higher collection efficiency than the $TE_{01}$ mode. In Fig. S13b we plot the contribution of both modes for a thick nanowire separately. We clearly see that for small time delays the $HE_{11}$ is the dominant lasing mode, whereas for larger time delays the $TE_{01}$ mode becomes the dominant mode, see Fig. S13b.

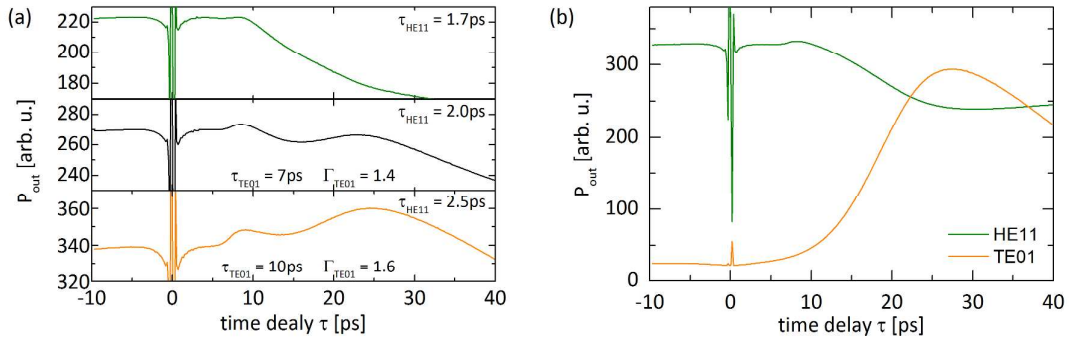


**Figure S13: Simulated double-pump response for two modes.** (a) Simulated double-pump response against time delay using the multimode laser rate equation model for thin (<150 nm), medium (~200 nm) and a thick (>200 nm) nanowire. (b) Total output of a thick nanowire separated in to the contributions of individual modes.

## References


[1] Casperson, L. *Journal of Applied Physics* **1975**, *46*, 5194–5201.

[2] Versteegh, M. A. M.; Kuis, T.; Stoof, H. T. C.; Dijkhuis, J. I. *Phys. Rev. B* **2011**, *84*, 035207.

[3] Sidiropoulos, T. P. H.; Röder, R.; Geburt, S.; Hess, O.; Maier, S. A.; Ronning, C.; Oulton, R. F. *Nat Phys* **2014**, *10*, 870–876.

[4] Zimmler, M.; Capasso, F.; Müller, S.; Ronning, C. *Semiconductor Science and Technology* **2010**, *25*, 024001.